Hindawi
Geofluids
Volume 2022, Article ID 6785373, 9 pages
https://doi.org/10.1155/2022/6785373

Research Article

Analysis and Application of Fractured Carbonate Dual-Media Composite Reservoir Model

Heng Song,[1] Yuan Hu,[2] Erhui Luo,[1] Congge He,[1] Xing Zeng,[1] and Shaoqi Zhang[2]

[1]*PetroChina Research Institute of Petroleum Exploration & Development, Beijing, China*
[2]*China University of Petroleum, Beijing, Beijing, China*

Correspondence should be addressed to Yuan Hu; hy7591@qq.com

Received 21 October 2021; Accepted 11 March 2022; Published 1 April 2022

Academic Editor: Wei Yu

Copyright © 2022 Heng Song et al. This is an open access article distributed under the Creative Commons Attribution License, which permits unrestricted use, distribution, and reproduction in any medium, provided the original work is properly cited.

Fractured carbonate reservoirs are different from conventional reservoirs and generally develop fractures. Conventional reservoir well test performance analysis can only obtain the formation parameters and discharge radius around a single well. For vertical wells in fractured carbonate reservoirs, we can establish a dual-porosity composite reservoir model for well testing interpretation and analysis based on the actual conditions of the reservoir and combined with geological knowledge. The model can be applied to formations with different reservoir properties in the near-well and far-well areas around a single well to analyze the fracture parameters (elastic reserve ratio and channeling coefficient) and the effective flow capacity of formation fluids in the two areas. On this basis, we use the interpretation of actual production wells to verify the accuracy of the model and analyze the influence of reservoir parameters and fracture parameters on the theoretical curve.

1. Introduction

Compared with conventional oil and gas reservoirs, fractured carbonate reservoirs generally have natural fractures, so one well has large controlled reserves and high production [1–7]. Carbonate reservoirs generally have two systems: matrix system and fracture system [8–16]. The matrix system is the storage space of oil and gas, and the fracture system is the migration channel of oil and gas in the formation [17–22]. It is of great significance to study the development degree of reservoir fractures and the channeling ability of matrix to fractures for formulating oil and gas field development plans and adjusting development performance.

In 1960, the former Soviet scholar Barenblatt et al. [23] established the dual-media seepage model and gave the general solution on the infinite plane, so as to establish the semilogarithmic curve chart of pressure drop well test and pressure recovery well test curve. In 1963, Warren and Root believed that the fractured carbonate reservoir can be divided into two systems [24]. The fracture system is simplified into vertical and orthogonal plane fractures, which cut the whole reservoir into small pieces of matrix rocks. The fluid flows through the matrix to the fractures and then into the wellbore. Two important parameters are used to characterize the condition of fractures and matrix in the reservoir, namely, elastic storage capacity ratio (ω) and channeling coefficient (λ). The elastic storage capacity ratio represents the space occupied by the fracture, and the channeling coefficient represents the conductivity of the fluid in the matrix to the fracture. At present, this model has been widely used in the study of oil and gas seepage in oil and gas reservoirs with natural fractures. In 1988, Houze et al. [25] studied the variation characteristics of bottom hole pressure of vertically fractured wells in dual-media reservoir. The research shows that parameters such as elastic storage capacity ratio, channeling coefficient, fracture half length, and fracture conductivity have varying degrees of influence on the variation of bottom hole pressure. In 2001, Verga [26] studied the bottom hole pressure response characteristics of a horizontal well in dual-media reservoir and drew the chart of the model by using Laplace transform and Stehfest numerical inversion method. In 2012, Yang et al. [27] researched that the dual-media well test curve represents the insignificant flow of fractures in the near-wellbore zone to the wellbore. In

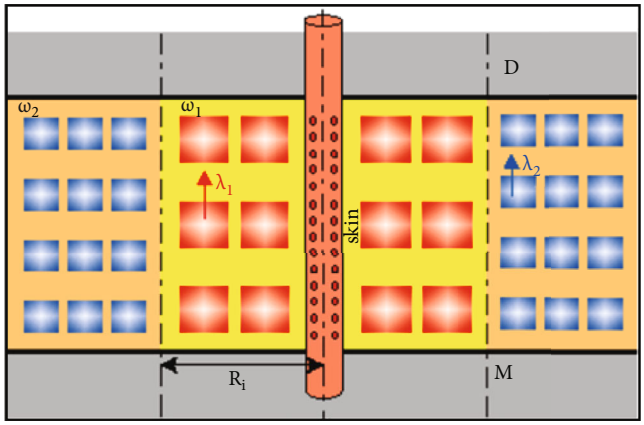

Figure 1: Schematic diagram of fluid flow in a dual-media composite reservoir model (cite from KAPPA).

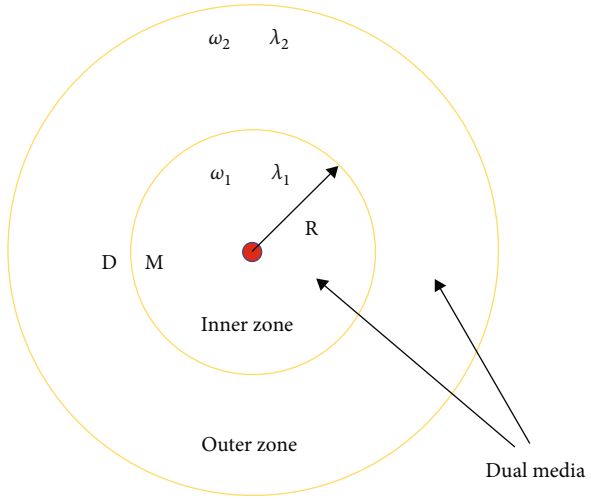

Figure 2: Dual-media composite reservoir model (cite from Feng's work [35]).

2014, Kuchuk and Biryukov [28] considered that Warren and Root model [29–31] is the result of idealizing the fracture length, width, thickness, distribution, and angle of natural fractures. This model has limitations in practical application, but it has not formed a practical and effective new model for the characterization of dual-media strata. In 2019, Zhang et al. [32] established a MFV model that considered the interaction of flow regimes in the matrix, discrete natural fractures, large fractures, and pores to simulate fluid flow in fractured-cavity reservoirs. In 2020, M. Wang et al. [33] combined the discrete fracture model (DFM) to simulate the local effects of discrete fractures and established a generalized multiscale multicontinuum model for fractured-cavity carbonate reservoirs. In 2021, Smeraglia et al. [34] developed a 3D discrete fracture network (DFN) model and characterized the fracture distribution in the low displacement (similar to 50 m) damage zone. In 2021, Li et al. [2] proposed a theoretical well test model that takes into account gravity effects and natural fractures connecting the caves and validated this type of reservoir.

Based on the oil-gas seepage theory, this study establishes a well test model suitable for different reservoir physical properties of single well near-well zone and far-well zone in fractured carbonate reservoir, makes a well test interpretation analysis for well A-21 in the fractured carbonate reservoir, and studies the influence of different parameters on the shape of double logarithm curve. This study provides important theoretical support for the inversion of fracture development, matrix channeling ability to fractures, and reservoir physical properties.

2. Method

2.1. Physical Model and Its Assumptions. Dual media is a porous medium with two types of pores: fracture and pore. Carbonate reservoir has a dual pore system with obvious fractures and pores. In the formation, due to the invasion of drilling fluid, acid fracturing, and gas injection, the properties of the reservoir near the wellbore change, making the reservoir properties in the near-wellbore zone and the far-well zone inconsistent. Therefore, a dual-media composite reservoir model is established to describe the reservoir conditions (see Figures 1 and 2).

The basic assumptions of the dual-media composite reservoir model are as follows:

(1) Fractured carbonate reservoirs are composed of matrix and fractures. Fluids in the fracture system flow directly into the wellbore. Fluids in the matrix system flow first into the fracture and then into the wellbore. The channeling flow between the fracture and the matrix system is pseudo-steady-state channeling

(2) The reservoir stratum is horizontal and equal thickness, the two layers are radially compounded, and the radius of the inner layer is R

(3) The fluid in the formation is an incompressible oil phase, and the influence of gravity and capillary force on the flow of crude oil in the formation is not considered

(4) The fluid in the fracture and matrix system conforms to Darcy's law of seepage and isothermal seepage

(5) The fluid flow in the wellbore considers the wellbore storage effect and the skin factor, where the wellbore storage factor is C and the skin factor is S

(6) The original formation pressure at the initial time of matrix system and fracture system in the formation is p_i

(7) There is no additional pressure drop at the transition interface between the inner and outer areas of the reservoir

2.2. Establishment and Solution of Mathematical Model. According to the assumptions, factors such as wellbore storage effect and skin effect are considered when establishing a dual-media composite reservoir model.

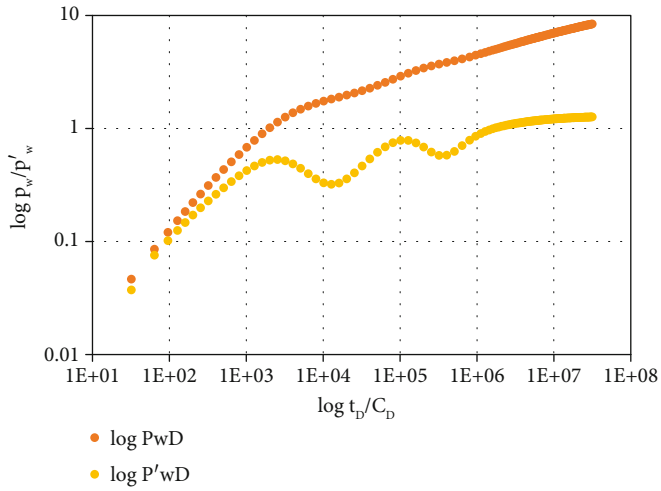

Figure 3: Theoretical double logarithm characteristic curve of dual-media composite reservoir model.

Table 1: basic parameter table.

Formation parameters	Result
k_1 (mD)	4
ω_1	0.05
λ_1	2×10^{-5}
k_2 (mD)	3.6
ω_2	0.05
λ_2	5.6×10^{-6}
C (m^3/MPa)	3
S	-5.7
R (m)	30
p_i (MPa)	50
h (m)	380
q (m^3/d)	200

In order to simplify the model and facilitate solution, dimensionless variables are first introduced:

$$p_{1fD} = \frac{K_{1f}h\left(p_i - p_{1f}\right)}{1.842 \times 10^{-3} qB\mu}, \tag{1}$$

where p_{1fD} is the dimensionless fracture pressure in the inner zone, k_{1f} is the fracture permeability in the inner zone, h is the effective stratum thickness, p_i is the initial formation pressure, p_{1f} is the fracture pressure in the inner zone, q is the ground yield, B is the crude oil volume factor, and μ is the crude oil viscosity.

$$p_{1mD} = \frac{K_{1f}h(p_i - p_{1m})}{1.842 \times 10^{-3} qB\mu}, \tag{2}$$

where p_{1mD} is the dimensionless matrix pressure in the inner zone and p_{1m} is the matrix pressure in the inner zone.

$$p_{2fD} = \frac{K_{1f}h\left(p_i - p_{2f}\right)}{1.842 \times 10^{-3} qB\mu}, \tag{3}$$

where p_{2fD} is the dimensionless fracture pressure in the outer zone, k_{2f} is the fracture permeability in the outer zone, and p_{2f} is the fracture pressure in the outer zone.

$$p_{2mD} = \frac{K_{1f}h(p_i - p_{2m})}{1.842 \times 10^{-3} qB\mu}, \tag{4}$$

where p_{2mD} is the dimensionless matrix pressure in the outer zone and p_{2m} is the matrix pressure in the outer zone.

$$p_{wfD} = \frac{K_{1f}h\left(p_i - p_{wf}\right)}{1.842 \times 10^{-3} qB\mu}, \tag{5}$$

where p_{wfD} is the dimensionless wellbore flow pressure and p_{wf} is the wellbore flow pressure.

$$t_D = \frac{3.6K_{1f}t}{(\phi VC_t)_1 \mu {r_w}^2}, \tag{6}$$

where t_D is the dimensionless time, t is time, r_w is the wellbore radius, and $(\phi VC_t)_1$ is the product of porosity, reservoir volume, and comprehensive elastic compressibility of the inner zone.

$$C_D = \frac{0.156C}{2\pi(\phi VC_t)_1 h{r_w}^2}, \tag{7}$$

where C_D is the dimensionless wellbore storage factor and C

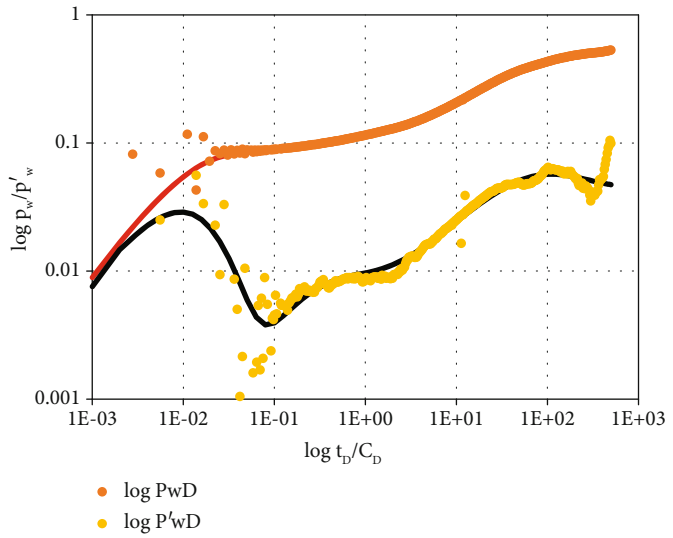

Figure. 4: Double logarithm curve fitting diagram of well A-21.

Table 2: Interpretation results of formation parameters of well A-21.

Formation parameters	Result
k_1 (mD)	20.5
ω_1	0.048
λ_1	1.15×10^{-5}
k_2 (mD)	1.8
ω_2	0.060
λ_2	8.83×10^{-5}
C (m^3/MPa)	1.61
S	-1.35
R (m)	108.5

is the wellbore storage factor.

$$r_D = \frac{r}{r_w}, \tag{8}$$

where r_D is the dimensionless radius and r is the radius.

The seepage differential equation is as follows:

$$\frac{1}{r_D}\frac{\partial}{\partial r_D}\left(r_D\frac{\partial p_{1fD}}{\partial r_D}\right) = \omega_1\frac{\partial p_{1fD}}{\partial t_{fmD}} + (1-\omega_1)\frac{\partial p_{1mD}}{\partial t_{fmD}}\left(1 \le r_D \le r_{fD}\right), \tag{9}$$

where ω_1 is the elastic storage capacity ratio of the inner zone and R_D is the dimensionless radius of the inner zone.

$$(1-\omega_1)\frac{\partial p_{1mD}}{\partial t_{fmD}} = \lambda_1\left(p_{1fD} - p_{1mD}\right), \tag{10}$$

where λ_1 is the channeling coefficient of the inner zone.

$$\frac{1}{r_D}\frac{\partial}{\partial r_D}\left(r_D\frac{\partial p_{2fD}}{\partial r_D}\right) = \eta_{12}\left[\omega_2\frac{\partial p_{2fD}}{\partial t_{fmD}} + (1-\omega_2)\frac{\partial p_{2mD}}{\partial t_{fmD}}\right]\left(r_{fD} \le r_D \le \infty\right), \tag{11}$$

where ω_2 is the elastic storage capacity ratio of the outer zone and η_{12} is the ratio of the conduction pressure coefficient of the inner zone to the outer zone.

$$(1-\omega_2)\eta_{12}\frac{\partial p_{2mD}}{\partial t_{fmD}} = \lambda_2\left(p_{2fD} - p_{2mD}\right). \tag{12}$$

The initial conditions are as follows:

$$\begin{aligned} p_{1fD}(r_D, 0) &= p_{1mD}(r_D, 0) = 0, \\ p_{2fD}(r_D, 0) &= p_{2mD}(r_D, 0) = 0. \end{aligned} \tag{13}$$

The internal boundary conditions are as follows:

$$\begin{aligned} C_D\frac{dp_{wfD}}{dt_{fmD}} - \left(r_D\frac{\partial p_{1fD}}{\partial r_D}\right)\Big|_{r_D=1} &= 1, \\ p_{wfD} &= \left(p_{1fD} - S\frac{\partial p_{1fD}}{\partial r_D}\right)\Big|_{r_D=1}. \end{aligned} \tag{14}$$

The connected surface conditions are as follows:

$$\begin{aligned} p_{1mD}(r_D = R_D) &= p_{2mD}(r_D = R_D), \\ p_{1fD}(r_D = R_D) &= p_{2fD}(r_D = R_D). \end{aligned} \tag{15}$$

The outer boundary condition is as follows:

$$\lim_{r_D \to \infty} p_{2mD} = \lim_{r_D \to \infty} p_{2fD} = 0. \tag{16}$$

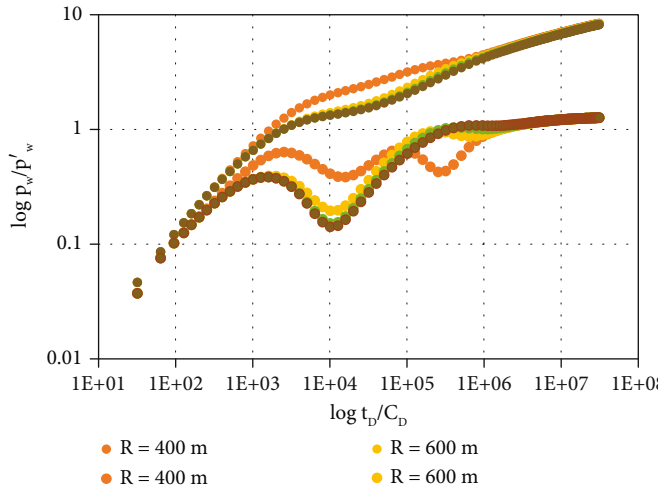

Figure 5: The influence of inner zone radius on pressure difference and pressure difference derivative curve.

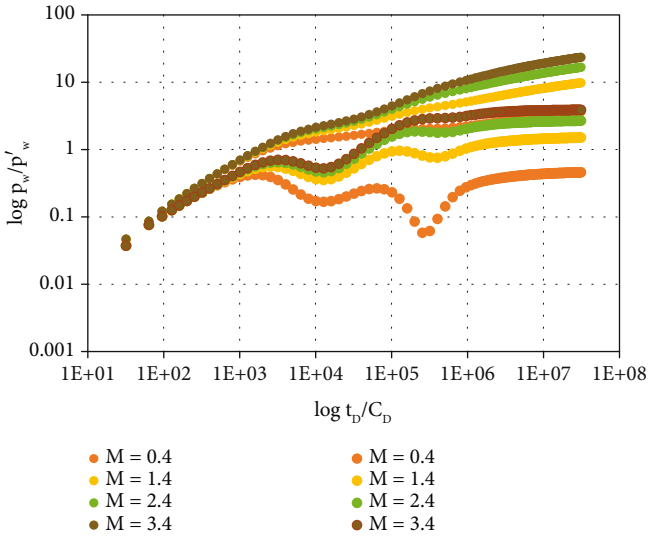

Figure 6: The influence of mobility ratio of the inner zone to the outer zone on pressure difference and pressure difference derivative curve.

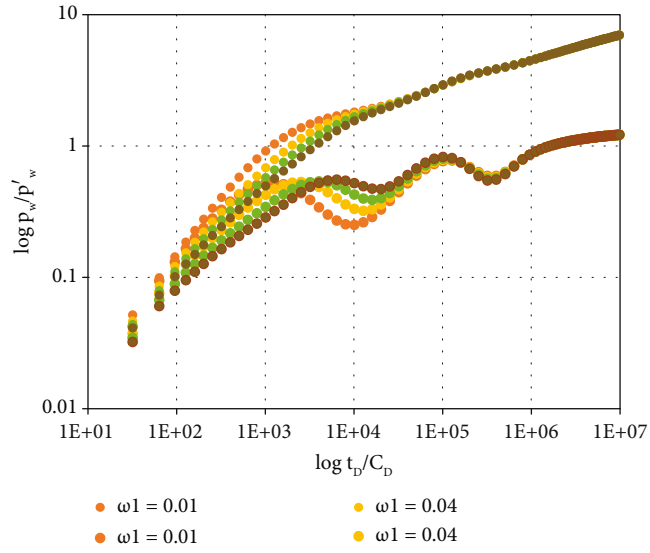

Figure 7: The influence of the elastic storage capacity ratio of the inner zone on pressure difference and pressure difference derivative curve.

Laplace transformation of dimensionless time t_{fmD} is performed on the above mathematical model to obtain the dimensionless pressure solution of the model in pull space (cite from Zhang's work [32]):

$$p_{wfD} = A_1\left[I_0\left(\sqrt{gf_1(g)}\right) - S\left(\sqrt{gf_1(g)}\right)I_1\left(\sqrt{gf_1(g)}\right)\right] + A_2\left[K_0\left(\sqrt{gf_1(g)}\right) + S\left(\sqrt{gf_1(g)}\right)K_1\left(\sqrt{gf_1(g)}\right)\right]. \quad (17)$$

In Equation (17),

$$f_1(g) = \frac{\omega_1(1-\omega_1)g + \lambda_1}{(1-\omega_1)g + \lambda_1}. \quad (18)$$

In Equation (17), $I_0(x)$ and $K_0(x)$ are the zero-order Bessel functions of the first kind and the second kind; $I_1(x)$ and $K_1(x)$ are the Bessel functions of the first order and the second kind; and A_1 and A_2 are the coefficients determined by internal and external boundary conditions.

2.3. Establishment and Characteristic Analysis of Bottom Hole Pressure Characteristic Curve Plate. Through Stehfest numerical inversion, the double logarithm characteristic curve of bottom hole pressure difference curve and pressure difference derivative curve of dual-media composite reservoir model can be obtained, as shown in Figure 3.

The basic parameters for calculating the characteristic curve are shown in Table 1.

As shown in Figure 3, according to the characteristics of double logarithm curve, the bottom hole pressure response characteristics of fractured carbonate dual-media composite reservoir can be divided into six flow stages:

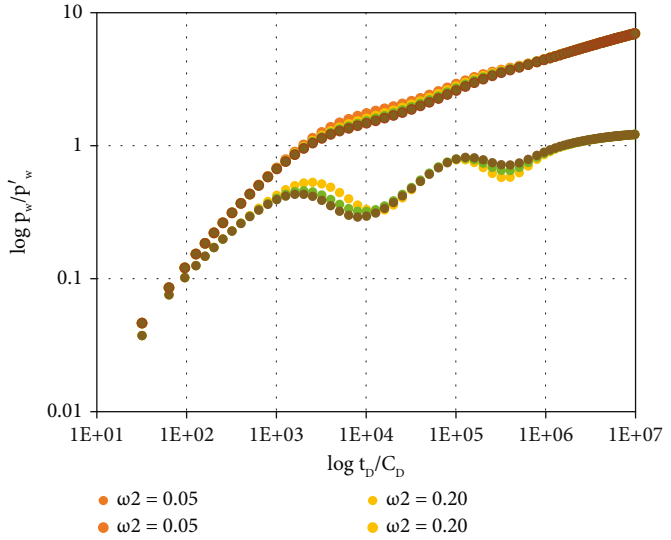

Figure 8: The influence of the elastic storage capacity ratio of the outer zone on pressure difference and pressure difference derivative curve.

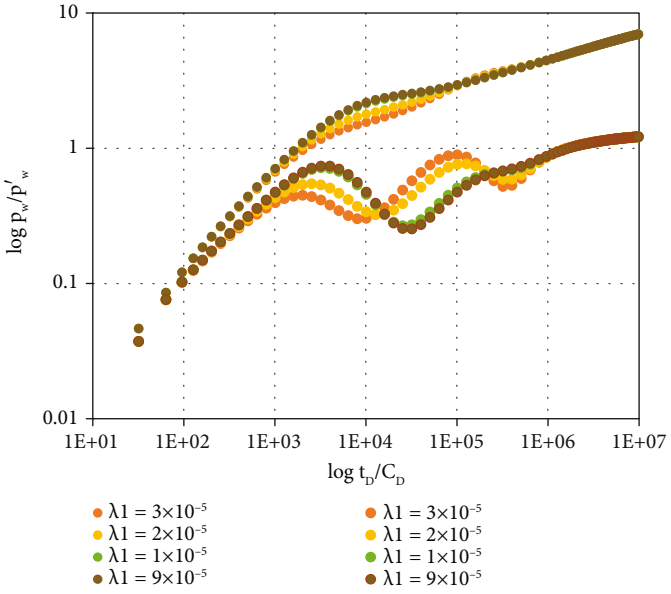

Figure 9: The influence of channeling coefficient of the inner zone on pressure difference and pressure difference derivative curve.

The first stage is wellbore storage stage. The pressure difference curve and pressure difference derivative curve coincide at this stage, and the slope is 1.

The second stage is skin effect stage. The pressure difference derivative curve shows the skin effect stage with the characteristics of "hump."

The third stage is the pseudo-steady-state channeling stage from the matrix system to the fracture system in the inner zone. The "concave" feature appears on the pressure difference derivative curve.

The fourth stage is flow transitional stage from the outer zone to the inner zone. Due to the interaction between different flow stages of the dual-media in the inner and outer zone, the shape of the pressure difference derivative curve is complex, and the position of the high point is not fixed. Due to the earlier transition phase, the radial flow in the inner zone is covered on the curve.

The fifth stage is the pseudo-steady-state channeling stage from the matrix system to the fracture system in the outer zone. The "concave" feature appears on the pressure difference derivative curve.

The sixth stage is plane radial flow stage in the outer zone. The horizontal section appears in the pressure difference derivative curve, which is a typical feature of radial flow in the outer system of the formation.

3. Model Verification

The research method is applied to the A-21 vertical well in the fractured carbonate reservoir block. The reservoir

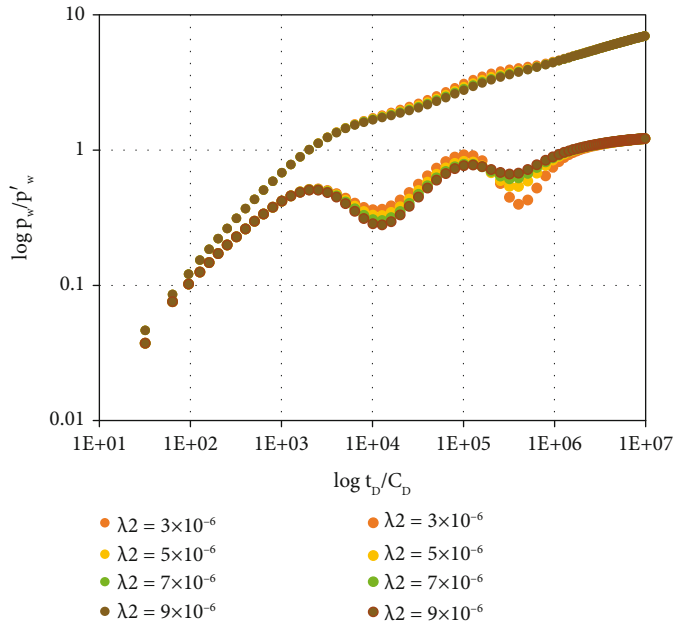

Figure 10: Influence curve of channeling coefficient of the outer zone on pressure difference and pressure difference derivative curve.

thickness is 12.55 m, the rock compressibility is 4.35×10^{-4} MPa^{-1}, its porosity is 0.0862, crude oil viscosity is 0.63, volume coefficient is 2.35 m^3/m^3, shut in pressure drop test is 500 h, and its medium depth of reservoir is 2248.13 m. Well A-21 was analyzed by the dual-media composite reservoir model, and the fitting diagram of the double logarithmic curve is shown in Figure 4.

The model is used to interpret the pressure test data of the well, and the inversion reservoir parameters are shown in Table 2.

4. Analysis on Influencing Factors of Bottom Hole Pressure Characteristic Curve

In order to study the change characteristics of the double logarithmic curve of the dual-media composite reservoir model, we analyzed the effects of the six parameters such as the radius of the inner(R), mobility ratio of the inner zone and outer zone (M), elastic storage capacity ratio of the inner zone (ω_1), elastic storage capacity ratio of the outer zone (ω_2), channeling coefficient of the inner zone (λ_1), and channeling coefficient of the outer zone(λ_2) on the shape characteristics of the differential pressure derivative curve.

4.1. The Radius of the Inner Zone. The radius of the inner zone is taken as 400 m, 600 m, 800 m, and 1000 m in turn. It can be seen from Figure 5 that the influence of the radius of the inner zone on the well test curve is mainly in the middle and end sections of the curve, which determines the time of flow transitional stage from the outer zone to the inner zone. The larger the inner radius, the later the flow transitional stage from the outer zone to the inner zone appears, the longer the fluid flow in the inner zone, and the less the curve shape of the inner zone flow stage is affected by the outer zone flow, so the inner zone flow stage is lower on the curve. At the same time, because the first "concave" and the second "concave" are similar, the change of the flow transitional stage from the outer zone to the inner zone curve will affect the shape of the two "concaves" at the same time and depth of depression of derivative curve.

4.2. Mobility Ratio of the Inner Zone to the Outer Zone. Mobility ratio of the inner zone to the outer zone is taken as 0.4, 1.4, 2.4, and 3.4. It can be seen from Figure 6 that mobility ratio of the inner zone to the outer zone reflects the ratio of fluid flow capacity of the inner zone to the outer zone. The influence of mobility ratio of the inner zone to the outer zone on the well test curve is mainly in the middle and later stages of the curve. The larger the mobility ratio of the inner and outer zones, the smaller the depression formed in the later transition section of the pressure difference derivative curve and the higher the horizontal section, the worse the morphological characteristics of the second concave, and the higher the horizontal section of radial flow in the outer zone, indicating that the fluid flow performance of the outer zone is poor.

4.3. Elastic Storage Capacity Ratio of the Inner Zone (ω_1). The elastic storage capacity ratio of the inner zone is taken as 0.01, 0.05, 0.09, and 0.14. It can be seen from Figure 7 that the influence of the elastic storage capacity ratio of the inner zone on the shape of the well test curve is mainly reflected in the middle section of the pressure difference derivative curve, which determines the concave degree of the first "concave" of the pressure difference derivative curve. The greater the elastic storage capacity ratio of the inner zone, the smaller the concave degree of the first "concave."

4.4. Elastic Storage Capacity Ratio of the Outer Zone (ω_2). The elastic storage capacity ratio of the outer zone is taken

as 0.05, 0.2, 0.35, and 0.5. It can be seen from Figure 8 that the influence of the elastic storage capacity ratio of the outer zone on the shape of the well test curve is mainly reflected in the middle section of the pressure difference derivative curve, which determines the concave degree of the second "concave" of the pressure difference derivative curve. The greater the elastic storage capacity ratio of the inner zone, the smaller the concave degree of the second "concave."

4.5. Channeling Coefficient of the Inner Zone (λ_1). The channeling coefficient of the inner zone is taken as 3.0×10^{-5}, 2.0×10^{-5}, 1.0×10^{-5}, and 9.0×10^{-6}. It can be seen from Figure 9 that the channeling coefficient of the inner zone determines the time when the first "concave" of the pressure difference derivative curve appears. The smaller the channeling coefficient of the inner zone value, the later the first "concavity" will appear. If the channeling coefficient of the inner zone continues to decrease, the quasiradial flow stage of the internal system may not appear and even the shape of the second "concave" is covered.

4.6. Channeling Coefficient of the Outer Zone (λ_2). The channeling coefficient of the outer zone is taken as 3.0×10^{-6}, 5.0×10^{-6}, 7.0×10^{-6}, and 9.0×10^{-6}. It can be seen from Figure 10 that the influence of the channeling coefficient in the outer zone on the well test curve is similar to the channeling coefficient in the inner zone. The value of the channeling coefficient of the outer zone determines the occurrence time of the second "concave." The smaller the value of the channeling coefficient, the more right the position of the second "concave."

5. Conclusion

Some fractured carbonate reservoirs have different reservoir conditions in the near-well zone and far-well zone. Therefore, we can establish a dual-media composite reservoir model explain and analyze the reservoir.

(1) The establishment of the theoretical curve chart found that the double logarithmic curve of the model can be divided into six stages: wellbore storage stage, skin effect stage, the pseudo-steady-state channeling stage, flow transitional stage from the outer zone to the inner zone, the pseudo-steady-state channeling stage from the matrix system to the fracture system in the outer zone, and plane radial flow stage

(2) Dual-media composite reservoir model is used to explain and analyze the reservoir conditions around Well A-21 of the fractured carbonate reservoir. The double logarithmic curve fits well, indicating that it is feasible to apply the model to explain the reservoir

(3) Through the sensitivity analysis of six parameters such as the radius of the inner(R), mobility ratio of the inner zone and outer zone (M), elastic storage capacity ratio of the inner zone (ω_1), elastic storage capacity ratio of the outer zone (ω_2), channeling coefficient of the inner zone (λ_1), and channeling coefficient of the outer zone (λ_2), the influence on the pressure difference derivative curve at each stage is obtained

Data Availability

The [PTA file and Microsoft Excel Worksheet] data used to support the findings of this study are available from the corresponding author upon request.

Conflicts of Interest

The authors declare that they have no conflicts of interest.

References

[1] R. Camacho-Velazquez, M. Vasquez-Cruz, R. Castrejon-Aivar, and V. Arana-Ortiz, "Pressure-transient and decline-curve behavior in naturally fractured vuggy carbonate reservoirs," *SPE Reservoir Evaluation & Engineering*, vol. 8, no. 2, pp. 95–112, 2005.

[2] L. Qingyu, D. Xin, T. Qingjun, Y. Xu, L. Peichao, and D. Lu, "A novel well test model for fractured vuggy carbonate reservoirs with the vertical bead-on-a-string structure," *Journal of Petroleum Science and Engineering*, vol. 196, p. 107938, 2021.

[3] C. Xing, H. Yin, K. Liu, X. Li, and J. Fu, "Well test analysis for fractured and vuggy carbonate reservoirs of well drilling in large scale cave," *Energies*, vol. 11, no. 1, p. 80, 2018.

[4] A. R. Adams, H. J. Ramey Jr., R. J. Burgess, and R. J. Burgess, "Gas well testing in a fractured carbonate reservoir," *Journal of Petroleum Technology*, vol. 20, no. 10, pp. 1187–1194, 1968.

[5] X. Du, Z. Lu, D. Li, Y. Xu, P. Li, and D. Lu, "A novel analytical well test model for fractured vuggy carbonate reservoirs considering the coupling between oil flow and wave propagation," *Journal of Petroleum Science and Engineering*, vol. 173, 2019.

[6] P. K. Dubey, S. Kumar, K. Havelia, and S. Yadav, "Integrated deterministic and predictive discrete fracture network modeling for an Eocene carbonate reservoir," *The Leading Edge*, vol. 38, 2019.

[7] A. H. Haghi, R. Chalaturnyk, and H. Ghobadi, "The state of stress in SW Iran and implications for hydraulic fracturing of a naturally fractured carbonate reservoir," *International Journal of Rock Mechanics and Mining Sciences*, vol. 105, pp. 28–43, 2018.

[8] L. Zhang, J. Zhang, Y. Zhao, and Y. Zhao, "Analysis of a finite element numerical solution for a nonlinear seepage flow model in a deformable dual media fractal reservoir," *Journal of Petroleum Science and Engineering*, vol. 76, no. 3-4, pp. 77–84, 2011.

[9] Y. Daiyin, Y. He, and X. Wang, "Numerical simulation for surfactant flooding in dual media low permeability reservoir," *International Journal of Applied Mathematics and Statistics™*, vol. 42, no. 12, 2013.

[10] X.-H. Tan, X.-P. Li, J.-Y. Liu, C. Tang, and J.-m. Li, "Pressure transient analysis of dual fractal reservoir," *Journal of Applied Mathematics*, vol. 2013, 9 pages, 2013.

[11] Z.-y. Liu, X.-d. Hu, Y.-j. Xiong, Y. Xue, and S. Liu, "Research on reservoir damage mechanism and protection technology of fracture- void dual medium reservoir," *International Journal of Energy Science*, vol. 1, 2011.

[12] G. Ba, S. Xu, and C. Zhang, "A double double-porosity model for wave propagation in patchy-saturated tight sandstone with

fabric heterogeneity," *ASEG Extended Abstracts*, vol. 2018, no. 1, pp. 1–6, 2018.

[13] Z.-G. Zhang, Y.-B. Liu, H.-T. Sun, W. Xiong, K. Shen, and Q.-B. Ba, "An alternative approach to match field production data from unconventional gas-bearing systems," *Petroleum Science*, vol. 17, no. 5, pp. 1370–1388, 2020.

[14] Z.-X. Xu, S.-Y. Li, B.-F. Li, D.-Q. Chen, Z.-Y. Liu, and Z.-M. Li, "A review of development methods and EOR technologies for carbonate reservoirs," *Petroleum Science*, vol. 17, no. 4, pp. 990–1013, 2020.

[15] L. I. Xizhe, L. U. Detang, L. U. O. Ruilan et al., "Quantitative criteria for identifying main flow channels in complex porous media," *Petroleum Exploration and Development*, vol. 46, no. 5, pp. 998–1005, 2019.

[16] C. Lina, L. Xiaoping, Z. Jiqiang, C. Luo, and X. Tan, "Dual-porosity model of rate transient analysis for horizontal well in tight gas reservoirs with consideration of threshold pressure gradient," *Journal of Hydrodynamics*, vol. 30, no. 5, pp. 872–881, 2018.

[17] Y. Zhang, L. Zeng, Q. Luo et al., "Influence of natural fractures on tight oil migration and production: a case study of Permian Lucaogou Formation in Jimsar Sag,Junggar Basin, NW China.," *Journal of Earth Science*, vol. 32, no. 4, pp. 927–945, 2021.

[18] H. Liu, S. Zhang, G. Song et al., "A discussion on the origin of shale reservoir inter-laminar fractures in the Shahejie Formation of Paleogene, Dongying Depression," *Journal of Earth Science*, vol. 28, no. 6, pp. 1064–1077, 2017.

[19] W. A. N. G. Dehai, K. A. N. G. Haiping, Z. H. A. O. Yanwei et al., "A study on accumulation and distribution of gas in southern Songliao Basin," *Global Geology*, vol. 16, no. 1, pp. 35–42, 2013.

[20] Z. H. A. I. Hongyu, X. CHANG, W. ZHU, X. LEI, and Z. XUE, "Study on anisotropy of Longmaxi shale using hydraulic fracturing experiment," *Science China Earth Sciences*, vol. 64, no. 2, pp. 260–277, 2021.

[21] G. U. Yifan, Z. H. O. U. Lu, J. I. A. N. G. Yuqiang, J. I. A. N. G. Chan, L. U. O. Mingsheng, and Z. H. U. Xun, "A model of hydrothermal dolomite reservoir facies in Precambrian dolomite, Central Sichuan Basin, SW China and its geochemical characteristics," *Acta Geologica Sinica*, vol. 93, no. 1, pp. 130–145, 2019.

[22] L. Guo, J. Zaixing, and F. Guo, "Mineralogy and fracture development characteristics of marine shale-gas reservoirs: a case study of lower Silurian strata in southeastern margin of Sichuan Basin, China," *China. Journal of Central South University*, vol. 22, no. 5, pp. 1847–1858, 2015.

[23] G. I. Barenblatt, I. P. Zheltov, and I. N. Kochina, "Basic concepts in the theory of seepage of homogeneous liquids in fissured rocks," *Journal of Applied Mathematics and Mechanics*, vol. 24, no. 5, pp. 1286–1303, 1960.

[24] J. E. Warren and P. J. Root, "The behavior of naturally fractured reservoirs," *Society of Petroleum Engineers*, vol. 3, no. 3, pp. 245–255, 1963.

[25] O. P. Houze, R. N. Horne, and H. J. Ramey, "Pressure-transient response of an infinite-conductivity vertical fracture in a reservoir with double-porosity behavior," *SPE Formation Evaluation*, vol. 3, no. 3, pp. 510–518, 1988.

[26] F. M. Verga, "Transient dual porosity behavior for horizontal wells case histories," *SPE Annual Technical Conference and Exhibition*, pp. 1–7, 2001.

[27] L. Yang, L. Tao, M. Xu, C. Wei, and F. Tao, "Well test curve analysis of YM2 fracture-cave carbonate," *Reservoir.Well Testing*, vol. 21, no. 6, 2012.

[28] F. Kuchuk and D. Biryukov, "Pressure-transient behavior of continuously and discretely fractured reservoirs," *SPE Reservoir Evaluation and Engineering*, vol. 17, no. 1, pp. 82–97, 2014.

[29] A. González-Calderón, L. X. Vivas-Cruz, U. Salmerón-Rodríguez, and U. Salmerón-Rodríguez, "Exact analytical solution of the telegraphic Warren and Root model," *Transport in Porous Media*, vol. 120, no. 2, pp. 433–448, 2017.

[30] S. Liu, S. Sang, Q. Zhu et al., "Triple medium physical model of post fracturing high-rank coal reservoir in southern Qinshui Basin," *Journal of Earth Science*, vol. 26, no. 3, pp. 407–415, 2015.

[31] B. Nœtinger, T. Estebenet, and T. Estebenet, "Up-scaling of double porosity fractured media using continuous-time random walks methods," *Transport in Porous Media*, vol. 39, no. 3, pp. 315–337, 2000.

[32] H. Zhang, W. Peng, P. Hao, and D. Menglin, "A heterogeneous model for simulating fluid flow in naturally fractured-vuggy carbonate reservoirs," *International Journal of Oil, Gas and Coal Technology*, vol. 20, no. 4, pp. 397–419, 2019.

[33] M. Wang, S. W. Cheung, E. T. Chung, M. Vasilyeva, and Y. Wang, "Generalized multiscale multicontinuum model for fractured vuggy carbonate reservoirs," *Journal of Computational and Applied Mathematics*, vol. 366, article 112370, 2020.

[34] L. Smeraglia, M. Mercuri, S. Tavani et al., "3D discrete fracture network (DFN) models of damage zone fluid corridors within a reservoir-scale normal fault in carbonates: multiscale approach using field data and UAV imagery," *Marine and Petroleum Geology*, vol. 126, article 104902, 2021.

[35] X. U. Feng, Y. U. Weiqiang, and L. I. Lun, "Well test interpretation method for buried hill reservoir based on dual medium composite gas reservoir model," *Well Testing*, vol. 28, no. 3, pp. 7–13, 2019.